Impact of lattice-shape moduli on band structure of photonic crystals

Arash Mafi*
Science and Technology, Corning Incorporated, Corning, New York 14831, USA
(Received 14 September 2007; published 28 March 2008)

We conduct a comprehensive study of the effect of the Bravais lattice-shape moduli on the band structure and in particular the band gap of photonic crystals. Unlike the conventional comparisons between triangular and rectangular photonic crystals, where the effect of the volume modulus is not separated, we rigorously decouple the volume modulus and determine the differences that can be attributed only to the shape of the lattice. We observe that the triangular lattice enjoys the largest band gap owing to its unique symmetry properties. We also show that the band gap decreases when the ratio of the lattice constants differs from unity. The use of an appropriate parametrization of the lattice-shape moduli combined with the inherent scaling invariance in the Maxwell equations allows us to cover Bravais lattices of all shape and volume moduli completely and without redundancy.

DOI: 10.1103/PhysRevB.77.115140 PACS number(s): 42.25.Bs

I. INTRODUCTION

Photonic crystals are of great interest in both fundamental and applied research.[1–3] Their applications span a wide range from classical to quantum optical systems, owing to their ability to control the flow of light and alter the spontaneous emission rate. The existence of photonic band gaps in these structures, caused by the periodic modulation of the refractive index, is central to their function in many of their applications. Consequently, the ability to control the size and location (in frequency space) of a band gap is quite important. There are various methods to control the band properties of photonic crystals. Selection of materials with different refractive indices and controlling the ratio and shape of these constituent materials in a unit cell are obvious methods. However, the underlying lattice geometry has a profound effect on the band properties of photonic crystals. Although it is known that the well-studied rectangular and triangular lattices give rise to different band properties, a systematic study of the implications of different lattice shapes has largely been ignored, so far. It is important to realize the relative ease of making different lattice shapes in photonic structures compared to electronic structures, where the lattice shapes are largely dictated by nature. A similar issue was addressed in another context in the study of the effect of shape moduli on the spectrum of the Kaluza-Klein gravitons arising from compactification of extra dimensions in string theory.[4–6] In this paper, we study some of the effects of the shape moduli of the underlying lattice on the optical behavior of photonic crystals. In particular, we show how the band structure and band gaps are affected. We restrict our paper to the case of two-dimensional (2D) photonic crystals, yet generalizations to 3D photonic crystals easily follow from our analysis.

Our observations can have important implications in the design of photonic-crystal-based devices. Control of the spontaneous emission rate by modifying the lattice geometry,[1] efficient bending of the light path in photonic crystals at any desired angle,[7] control of the dispersion properties of slow light propagating in optical buffers,[8] and alteration of the enhanced transmission frequency peak through subwavelength holes in metal films[9] are possible applications.

II. MODULAR SYMMETRY

In Fig. 1, we show an example of a photonic crystal that is made from a periodic array of cylindrical rods embedded within a dielectric material with different permittivity. The two-dimensional periodic Bravais lattice Ω of the photonic crystal is defined by a pair of generator vectors $\mathbf{\Lambda}_1, \mathbf{\Lambda}_2$ making a relative angle θ where $\Omega = \{ m_1\mathbf{\Lambda}_1 + m_2\mathbf{\Lambda}_2 | m_1, m_2 \in \mathbb{Z}\}$. The same lattice can be characterized (redundantly) by an infinite pair of "equivalent" generators where each pair relates to another by an element of the modular group. Ω may alternatively be represented by the pair of the volume modulus ("Kähler modulus") $V = \Lambda_1\Lambda_2 \sin\theta$ and the shape modulus ("complex modulus") $\tau = (\Lambda_2/\Lambda_1)e^{i\theta}$.[10] The mentioned redundancy is best characterized in the complex plane of τ. For every lattice, a basis can always be chosen in the fundamental domain $\mathcal{D}$ highlighted by gray in Fig. 2, and each point outside $\mathcal{D}$ can always be mapped by a modular transformation to a point in $\mathcal{D}$. The fundamental domain is given by $\mathcal{D}_1 \cup \mathcal{D}_2 \in \mathbb{C}^+$ where

$$\mathcal{D}_1 = |\tau| > 1, \quad |\mathrm{Re}(\tau)| < 1/2, \tag{1}$$

$\mathcal{D}_2$ is the darker boundary line, and $\mathbb{C}^+$ is the upper half complex plane. We note that all the points inside the fundamental domain $\mathcal{D}$ are associated with distinct lattices, while any point outside $\mathcal{D}$ represents a redundant description of a lattice inside $\mathcal{D}$. We can therefore remove the redundancy associated with the τ parametrization by limiting our study to

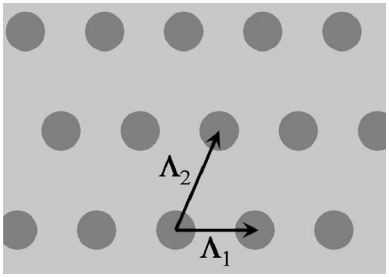

FIG. 1. Two-dimensional periodic lattice of rods within a dielectric of different-index material.

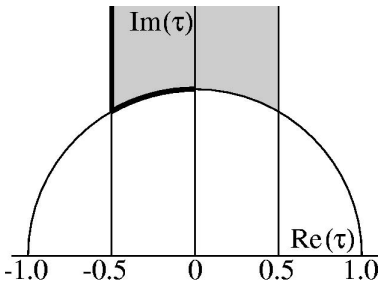

FIG. 2. Complex plane of the shape modulus τ: the fundamental domain is marked with a darker color.

$\mathcal{D}$. In fact, a full characterization of the optical effects of the shape moduli is possible by studying $\mathcal{D}$ for a fixed value of volume V. The reason is that, once a photonic crystal is studied for all frequencies at fixed V, any other value of the volume modulus can be accessed using the scale invariance in Maxwell's equations. In other words, the dependence on the volume modulus is trivially determined once the problem of the shape modulus is fully solved at a fixed volume. In a general two-dimensional periodic lattice (for which Fig. 1 is a particular example), the permittivity is invariant under the following transformations:

$$\epsilon(x+\Lambda_1,y)=\epsilon(x+\Lambda_2\cos\theta,y+\Lambda_2\sin\theta)=\epsilon(x,y). \quad (2)$$

Without loss of generality, we have assumed that $\mathbf{\Lambda}_1$ is along the x axis. For simplicity, we also ignore any magnetic response of the constituent materials. The spatial part of the electric field (using Bloch's theorem) can be written as

$$\mathbf{E}(x,y)=\mathbf{E}_{\{k\}}(x,y)\exp i\left[k_1x+\left(\frac{k_2}{\sin\theta}-\frac{k_1}{\tan\theta}\right)y\right], \quad (3)$$

where $\mathbf{E}_{\{k\}}$ is invariant under the same transformations of Eq. (2) and is a solution of

$$[-D_{\{k\}}^2+\epsilon(x,y)\omega^2]\mathbf{E}_{\{k\}}(x,y)=0,$$

$$D_{\{k\}}=\left[\nabla+ik_1\hat{x}+i\left(\frac{k_2}{\sin\theta}-i\frac{k_1}{\tan\theta}\right)\hat{y}\right]\times \quad (4)$$

The cross sign in Eq. (4) is interpreted as the curl operator when used with ∇ and as an exterior vector product for the rest of the terms. The decomposition in Eq. (3) follows the standard reciprocal lattice vector calculations where the exponent is transformed by $ik_1\Lambda_1$ and $ik_2\Lambda_2$ under the transformations of Eq. (2). The band properties of the photonic crystal can be fully studied by solving Eq. (4) in the first Brillouin zone of the k space, which is given by

$$-\pi/\Lambda_i<k_i\leq\pi/\Lambda_i, \quad i=1,2. \quad (5)$$

Point symmetries can be exploited to further reduce the interesting region of the k space to the irreducible Brillouin zone. However, we caution that a general modular lattice has "lower" spatial symmetries than the often studied triangular or rectangular lattices, and the irreducible Brillouin zone is no longer a simple triangle. The first Brillouin zone of a general two-dimensional lattice is shown in Fig. 3; it lies inside the polygon marked by points A_i, $i=1-6$, and Γ is the central point. The first Brillouin zone is the smallest area entirely enclosed by lines that are the perpendicular bisectors of the reciprocal lattice vectors drawn from the origin. For example, A_2-A_3 and A_5-A_6 are perpendicular bisectors of the dotted lines connecting the origin to the corner lattice points. The irreducible Brillouin zone is also a polygon, half the size of the above polygon, marked by the points Γ,A_1,A_2,A_3,A_4.

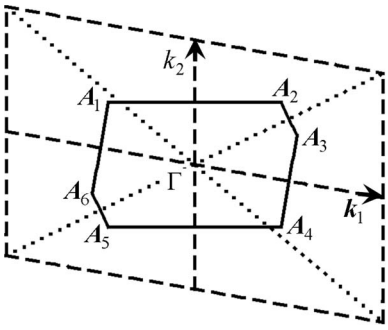

FIG. 3. Reciprocal lattice; the irreducible Brillouin zone is the polygon marked by points Γ,A_1,A_2,A_3,A_4.

III. EXAMPLES

In the examples presented below, we consider the photonic crystal in Fig. 1 where rods of radius R and refractive index ϵ_r are periodically embedded within the background dielectric material of permittivity ϵ_s. Since we are interested in isolating the effect of the shape modulus and have also argued that it is sufficient to study the photonic crystal at a particular volume for all frequencies, we fix our volume to be the volume of a square lattice whose sides are of length Λ_0, i.e., $V=\Lambda_0^2$, and we have

$$\Lambda_2=|\tau|\Lambda_1=\sqrt{V|\tau|/\sin\theta}. \quad (6)$$

We initially consider the special case of $|\tau|=1$. The band structure of a photonic crystal can be easily determined by finding the solutions of Eq. (4). This can be achieved using various numerical techniques such as the plane-wave expansion method of Ref. 11, which we have used in this paper.

We first compute the band diagram for the TM polarization for values of $\epsilon_s=1$ and $\epsilon_r=13$ in the case where $|\tau|=1$. The band diagram for the lowest two frequency bands is plotted in Fig. 4 around the perimeter of the irreducible Brillouin zone illustrated in Fig. 3 for $R/\Lambda_0=0.2$ and $\theta=30°,60°,90°$ as solid, dashed, and dot-dashed lines, respectively. Similarly to the more familiar cases of triangular and rectangular lattices, it is sufficient to study the band structure of the lattice only around the perimeter of the irreducible Brillouin zone to reveal the band gaps. It is clear from Fig. 4 that $\theta=60°$ gives the largest band gap in this case. This is not surprising considering the fact that a triangular lattice (with equal sides) is special; enjoying the highest symmetry and being a fixed point of the modular group corresponding to $\tau=e^{i\pi/3}$ (the square lattice corresponding to $\tau=i$ is the other fixed point). We plot in Fig. 5 the frequency band gap of the same lattice as a function of the lattice angle $\theta\leq 90°$. We have chosen three cases of $R/\Lambda_0=0.2,0.3,0.4$,

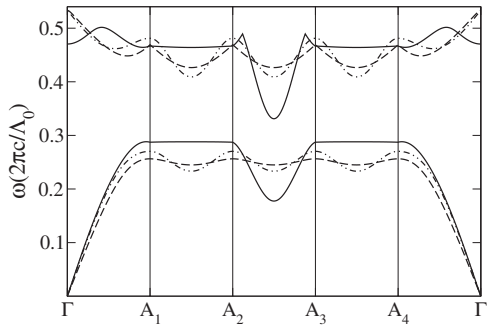

FIG. 4. TM band diagram for $\theta=30°, 60°, 90°$ as solid, dashed, and dot-dashed lines, respectively.

where the top dotted region enclosed in the solid line relates to $R/\Lambda_0=0.2$ with some overlap with the middle dotted region of $R/\Lambda_0=0.3$. The lowest dotted area relates to $R/\Lambda_0=0.4$ which also has some overlap with the middle dotted region of $R/\Lambda_0=0.3$. It is clear again from Fig. 5 that the triangular lattice enjoys the largest band gap in each case. Similarly, we plot the band gap of the same lattice for TE polarization in Fig. 6 ($R/\Lambda_0=0.3$ is the top dotted region), where the triangular lattice has the largest band gap again. We note that $R/\Lambda_0=0.2$ did not correspond to any band gaps in this case. We note that the band gap is symmetric under $\mathrm{Re}(\tau)\rightarrow-\mathrm{Re}(\tau)$ since the physics of the photonic crystal is invariant under a mirror transformation around its x axis. This is the reason we have chosen $\theta\leq 90°$, where θ and $180°-\theta$ give identical results. It is notable that the rods shown in Fig. 1 would overlap if $\theta<\theta_{\min}$ where

$$\theta_{\min}=2\tan^{-1}2\left(\frac{R}{\Lambda_0}\right)^2, \tag{7}$$

and we have used Eq. (6) with $|\tau|=1$ in deriving Eq. (7). The calculated value of $\theta_{\min}$ in Figs. 5 and 6 is smaller than any angle in the highlighted band gap region. We now relax the condition $|\tau|=1$ and study the TM band gap for $R/\Lambda_0=0.2$ in the τ plane in Fig. 7. The band gap is maximum around the corners of the fundamental region corresponding to the equilateral triangular lattice and decreases when $|\tau|$ increases.

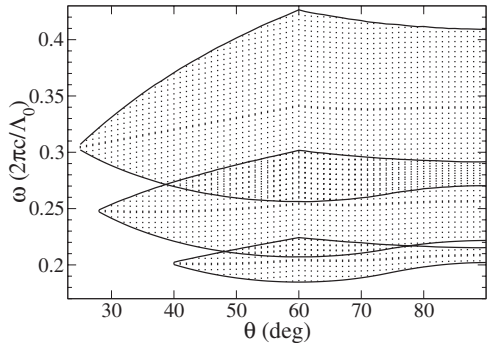

FIG. 5. TM band gaps for $R/\Lambda_0=0.2, 0.3, 0.4$. The top dotted region enclosed by the solid line relates to $R/\Lambda_0=0.2$ with some overlap with the middle dotted region of $R/\Lambda_0=0.3$. The lowest dotted area relates to $R/\Lambda_0=0.4$ and also has some overlap with the middle dotted region of $R/\Lambda_0=0.3$.

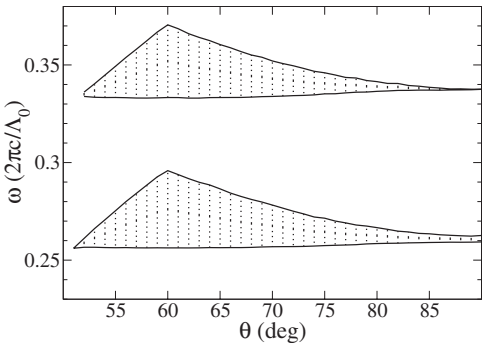

FIG. 6. TE band gaps for $R/\Lambda_0=0.3, 0.4$. The top dotted region enclosed in the solid line relates to $R/\Lambda_0=0.3$.

The symmetry around the vertical axis is expected, as explained earlier.

In order to get a more concrete understanding of the effects of the shape moduli, it would be helpful to look for some simple analytical approximations that directly illustrate how they impact the band structure of photonic crystals. We showed that, by solving Eq. (4), we can access the band structure, and this equation must usually be solved numerically. The lattice-periodic solutions $\mathbf{E}_{\{k\}}$ can be expanded in terms of Bloch waves $\psi_{\{m\}}$,

$$\mathbf{E}_{k_1,k_2}=\sum_{m_1,m_2=-\infty}^{\infty}\mathbf{C}_{k_1,k_2}^{m_1,m_2}\psi_{m_1,m_2}, \tag{8}$$

where $\mathbf{C}_{\{k\}}^{\{m\}}$ are the (vectorial) expansion coefficients and

$$\psi_{\{m\}}=\exp 2\pi i\left[\frac{m_1}{\Lambda_1}x+\left(\frac{m_2}{\Lambda_2\sin\theta}-\frac{m_1}{\Lambda_1\tan\theta}\right)y\right]. \tag{9}$$

The subscript $\{m\}$ in Eq. (9) represents the integers m_1 and m_2 of the discrete Fourier expansion that respects the periodicity of the lattice. In particular, $\psi_{\{m\}}$ satisfies Eq. (4) in the limit of a spatially constant $\epsilon(x,y)=\epsilon_s$ for which we get the dispersion equation

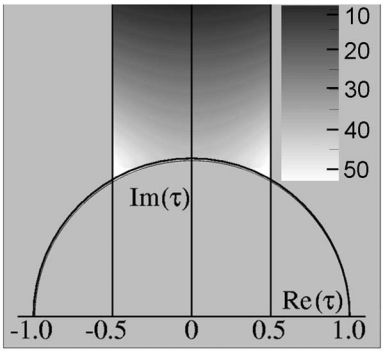

FIG. 7. Density plot of the TM band gap width normalized by the band gap center frequency (%) for $R/\Lambda_0=0.2$ in the complex τ plane for $0\leq\mathrm{Im}(\tau)\leq 2$. The normalized band gap width ranges from ~10% to ~50%, as shown on the sidebar.

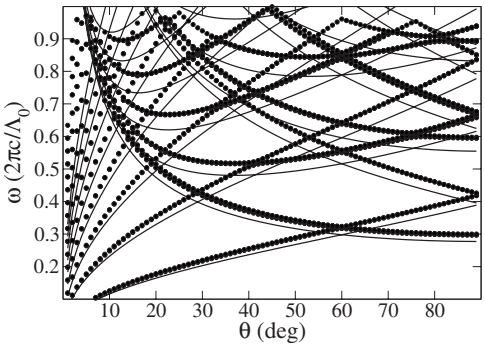

FIG. 8. Γ-point frequencies: solid lines are from Eq. (11) for $\epsilon_s=13$ and dotted lines represent the TE-polarization numerical solution for $R/\Lambda_0=0.2$ and $\epsilon_r=11$.

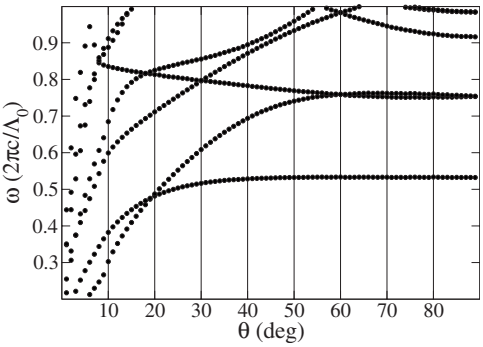

FIG. 9. Γ-point frequencies for TE-polarization numerical solution with $R/\Lambda_0=0.2$, $\epsilon_s=13$, and $\epsilon_r=1$.

$$\epsilon_s\omega^2=\left(\frac{2\pi m_1}{\Lambda_1}+k_1\right)^2+\left(\frac{2\pi m_2}{\Lambda_2\sin\theta}-\frac{2\pi m_1}{\Lambda_1\tan\theta}+\frac{k_2}{\sin\theta}-\frac{k_1}{\tan\theta}\right)^2. \quad (10)$$

Equation (10) is nothing but an alternative way of writing the usual parabolic dispersion relation of a plane wave in two dimensions, where we have imposed a "seemingly unnecessary" lattice-periodic boundary condition on the uniform dielectric medium. The lattice-periodic boundary condition is required as soon as we introduce (not necessarily small) perturbations in the refractive index of the uniform dielectric medium. Lets now consider the dependence of frequencies at point Γ $(k_1,k_2=0)$, where Eq. (10) can be simplified to

$$\left(\frac{V}{4\pi^2}\right)\epsilon_s\omega^2_{m_1,m_2}=\frac{1}{\sin\theta}(|\tau|m_1^2+|\tau|^{-1}m_2^2-2m_1m_2\cos\theta). \quad (11)$$

The special case of $|\tau|=1$ in Eq. (11) for $\epsilon_s=13$ is plotted in Fig. 8 as solid lines for several values of m_1 and m_2 compared with the actual TE-polarization numerical solution for $R/\Lambda_0=0.2$ with $\epsilon_s=13$ and $\epsilon_r=11$ as the dotted line. It is clear that, in this case where the refractive index of the rods is not considerably different from the background refractive index, the quantitative agreement is substantial. We also plot the case of a high-refractive-index contrast where $\epsilon_r=1$ in Fig. 9 and show how the presence of a large index contrast modifies the simplified picture portrayed by Eq. (10).

In summary, we showed the considerable impact of the shape of the underlying Bravais lattice in photonic crystals. We presented a modular characterization of the nontrivial irreducible Brillouin zone of a general Bravais lattice and properly separated the effect of the volume modulus. This is in contrast to the conventional studies of the differences between triangular and rectangular photonic crystals, where the effect of the volume modulus is not properly separated by using equal lattice constants, making the volume rescaling an important factor in the observed differences. We showed that the triangular lattice enjoys the largest band gap owing to its unique symmetry properties and also showed that the band gap decreases when the ratio of the lattice constants differs from unity. We hope that our observations illustrate the importance of the shape of the underlying lattice geometry in photonic crystals and prompt further investigations.

ACKNOWLEDGMENTS

The author would like to acknowledge Karl Koch of Corning, Inc. for important corrections and suggestions.

*mafi@corning.com

[1] E. Yablonovitch, Phys. Rev. Lett. **58**, 2059 (1987).
[2] S. John, Phys. Rev. Lett. **58**, 2486 (1987).
[3] J. D. Joannopoulos, P. R. Villeneuve, and S. Fan, Nature (London) **386**, 143 (1997).
[4] K. R. Dienes, Phys. Rev. Lett. **88**, 011601 (2001).
[5] K. R. Dienes and A. Mafi, Phys. Rev. Lett. **88**, 111602 (2002).
[6] K. R. Dienes and A. Mafi, Phys. Rev. Lett. **89**, 171602 (2002).
[7] A. Mekis, J. C. Chen, I. Kurland, S. Fan, P. R. Villeneuve, and J. D. Joannopoulos, Phys. Rev. Lett. **77**, 3787 (1996).
[8] M. Notomi, K. Yamada, A. Shinya, J. Takahashi, C. Takahashi, and I. Yokohama, Phys. Rev. Lett. **87**, 253902 (2001).
[9] A. Krishnan, T. Thio, T. J. Kim, H. J. Lezec, T. W. Ebbesen, P. A. Wolff, J. Pendry, L. Martin-Moreno, and F. J. Garcia-Vidal, Opt. Commun. **200**, 1 (2001).
[10] M. Nakahara, *Geometry, Topology and Physics* (IOP Publishing, London, 1990).
[11] S. G. Johnson and J. D. Joannopoulos, Opt. Express **8**, 173 (2001).